CHAPTER 6

CONCLUSIONS

The impact of processing conditions on the ceramic dielectric properties was studied by investigating P1 and P2 specimens whose compositions are of the form xBa($Mg_{1/3}Nb_{2/3}$)O_3-(1-x)$BaTiO_3$ (where $0 \leq x \leq 0.07$). The drawn conclusions are as following:

1. Overall, P1 ceramics exhibited higher dielectric constant and better diffuse phase transition compared to P2 ceramics indicating that the P1 process should be more appropriate in manufacturing MLC capacitors.
2. The maximum dielectric constant obtained for P1 and P2 specimens was 40,000 (x = 0.02, T_c ~ 98 °C) and 13,300 (x = 0.05, T_c ~ 18 °C), respectively. In particular, when x = 0.04, the P1 samples depicted X7R characteristic, i.e., ε_r = 13,000 at 25°C with variation ~ 6 % over the temperature range of −50°C-170°C.
3. The coexistence of tetragonal and cubic phases was found in samples with small contents of additive ($x \leq 0.04$) and at x = 0.05, the tetragonal-cubic transformation occurred at room temperature in both processes. For x = 0.07 P1 ceramics transformed to rhombohedral phase at room temperature.
4. The lattice parameter, c/a, decreased with increasing x for both P1 and P2 samples. However, P1 ceramics possess a bit higher order of tetragonality compared to P2 ceramics.

5. The average density of P1 and P2 samples was about 95% and 93% of the theoretical value respectively. For $x = 0.04$, P2 samples showed cracking due to internal stress originated from cubic-tetragonal transformation.

6. Grain growth inhibition is significant at $x = 0.04$ and the average grain size tends to decrease with increasing x. Moreover, the second phase was found at grain boundary. The thickness of the second phase in P2 samples was generally larger compared to that of P1 samples.

7. EPMA data identified the second phase in P1 ceramics as $Ba_6Ti_{17}O_{40}$ and as the coexistence of $Ba_6Ti_{17}O_{40}$ and $Ba_4MgTi_{11}O_{27}$ in P2 ceramics.

8. The dissipation factor (tanδ) of BMN-BT ceramics from both processes was slightly higher than that of the undoped BT at room temperature and increased markedly at temperatures > 150 °C. The highest value of tanδ was 0.085 and 0.46, found at $x = 0.02$ and 0.04, for P1 and P2 samples respectively.

PART I: Effects of sintering aids on (100-x) $0.02Ba(Mg_{1/3}Nb_{2/3})O_3$-$0.98BaTiO_3$-$x Bi_2O_3/Li_2CO_3$ ceramics, where $2 \leq x \leq 10$ (S1 Ceramics).

9. The Bi_2O_3/Li_2CO_3 sintering aids reduced the sintering temperature to < 1000 °C for $x \geq 3$, and the density increased to 5.9 g/cm^3 from 5.8 g/cm^3 of BMN-BT.

10. The XRD data revealed the coexistence of cubic and tetragonal phases when $3 \leq x \leq 6$ and the transformation to rhombohedral phase when $x = 10$.

11. The presence of secondary phases, mainly $LiBa_4Bi_3O_{11}$ and $Ba_2Bi_4Ti_5O_{18}$, was found for $x \geq 3$ whereas the grain growth inhibition was also observed. The

ceramics consequently contained smaller grains with more uniform microstructure.

12. T_c shifted to lower temperature, 88 °C-58 °C, with increasing x ($0 \leq x \leq 6$).

13. The highest ε_r obtained was 11,880 when $x = 3$ and $T_s = 950$ °C.

PART II: Effects of sintering aids on (100-*x*-*y*) $0.02Ba(Mg_{1/3}Nb_{2/3})O_3$-$0.98BaTiO_3$ - xBi_2O_3/Li_2CO_3-yPbO ceramics (S2 Ceramics).

14. The sintering temperature could be lowered from around 1300°C to 900°C by adding Bi_2O_3/Li_2CO_3 and PbO. However, the density was slightly decreased from 5.8 g/cm^3 of pure $0.02Ba(Mg_{1/3}Nb_{2/3})O_3$-$0.98BaTiO_3$ to 5.6 g/cm^3.

15. Grain growth suppression was observed and as a consequence the average grain sizes of all specimens were not larger than 6 μm but the grain size distribution was quite homogeneous.

16. The transformation from ferroelectric to paraelectric phase occurred when flux concentration was double the amount used to cause the ceramic ferroelectric state.

17. In general, the ε_r values of the S2 ceramics were considerably decreased except for the $96.5[0.02Ba(Mg_{1/3}Nb_{2/3})O_3$-$0.98BaTiO_3]$-$2.63Bi_2O_3/Li_2CO_3$-0.87PbO ceramic (Sample B) whose ε_r was relatively high (> 16,500) and invaried over the temperature range around 100°C to 225C°.

18. The dissipation factor (at 1kHz) was ~ 2.5 at room temperature but increased abruptly and substantially at temperature ~ 150°C.

SUGGESTIONS FOR FURTURE WORK

1. The dielectric constant-temperature characteristics of xBa($Mg_{1/3}Nb_{2/3}$)O_3-(1-x)$BaTiO_3$, where x = 0.02-0.04 and prepared by P1 processing, exhibited the diffuse phase transitions which were proposed to be due to the core-shell microstructure with concentration gradients of elements in a grain. This proposal has yet to be confirmed by the TEM study of the ceramics.
2. As the 0.04Ba($Mg_{1/3}Nb_{2/3}$)O_3-0.96$BaTiO_3$ ceramic was found to meet the X7R specifications and results obtained for the 96.5[0.03Ba($Mg_{1/3}Nb_{2/3}$)O_3-0.97$BaTiO_3$]-2.63[Bi_2O_3/Li_2CO_3]-0.87PbO composition are as shown in Figure A below, another interesting composition (likely to yield the properties required for MLC application) suggested for further study is the 96.5[0.03Ba($Mg_{1/3}Nb_{2/3}$)O_3-0.97$BaTiO_3$]-2.63[Bi_2O_3/Li_2CO_3]-0.87PbO.

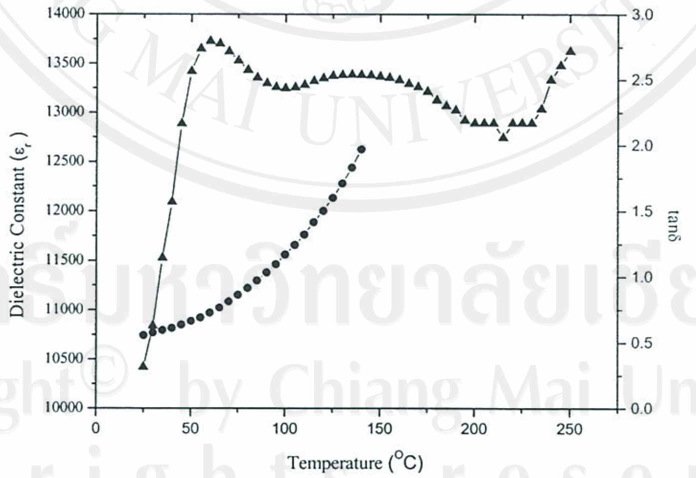

Figure A Dielectric constant at (1 kHz) as a function of temperature for 96.5[0.03Ba($Mg_{1/3}Nb_{2/3}$)O_3-0.97$BaTiO_3$]-2.68[Bi_2O_3/Li_2CO_3]-0.87PbO ceramics sintered at 900°C.

3. The thermal etching technique is more appropriate than the chemical etching in investigating the synthesized ceramics.
4. Effects of the PbO sintering aid on BMN-BT ceramics should be studied in more details.